PHYSICAL REVIEW A VOLUME 39, NUMBER 11 JUNE 1, 1989

Electron exchange in collisions with O_2 and NO

J. M. Ratliff, G. H. Rutherford, F. B. Dunning, and G. K. Walters
Department of Physics and the Rice Quantum Institute, Rice University, Houston, Texas 77251

(Received 13 February 1989)

Rate constants for electron exchange in collisions between thermal-energy, spin-polarized electrons and O_2 and NO have been measured using a flowing-helium afterglow apparatus. The measured rate constants, $\sim 10^{-10}\ \mathrm{cm}^3\,\mathrm{sec}^{-1}$, are substantially smaller than those for electron exchange in collisions with hydrogen or alkali-metal atoms.

Collisions of spin-polarized electrons with molecular targets such as O_2 or NO that are not spin singlets can lead to a degradation in electron polarization via electron exchange reactions of the type

$$e^-(\uparrow)+O_2\begin{Bmatrix} M_S=0 \\ M_S=-1\end{Bmatrix}\rightarrow e^-(\downarrow)+O_2\begin{Bmatrix} M_S=+1 \\ M_S=0\end{Bmatrix},$$
$$e^-(\uparrow)+\mathrm{NO}\{M_S=-\tfrac{1}{2}\}\rightarrow e^-(\downarrow)+\mathrm{NO}\{M_S=+\tfrac{1}{2}\}, \qquad (1)$$

where M_S denotes the spin-projection quantum number for the molecule. Such exchange reactions are frequently studied, at electron energies greater than a few electron volts, using beam techniques,[1,2] but few experimental data are available at thermal collision energies.[3,4] In the present work a flowing-helium afterglow apparatus has been used to investigate electron exchange in thermal-energy collisions with O_2 and NO. The measured rate constants, $\sim 10^{-10}\ \mathrm{cm}^3\,\mathrm{sec}^{-1}$, are substantially smaller than those for spin exchange in collisions with hydrogen[5] or alkali-metal atoms.[3,4]

The present apparatus is shown schematically in Fig. 1.[6,7] Briefly, a microwave discharge is used to generate $\mathrm{He}(2\,^3S)$ metastable atoms in a flowing-helium afterglow. The $2\,^3S$ atoms are optically pumped[7] to preferentially populate either the $M_J'(M_S')=+1$ or -1 magnetic sublevels. CO_2 is then introduced into the flow tube resulting in the production of polarized electrons through Penning ionization.[8] These electrons are rapidly thermalized by collisions and are then allowed to interact with either O_2 or NO introduced downstream. The degradation in polarization that results from electron-exchange reactions is determined by extracting electrons from the flow tube through a differentially pumped aperture and measuring their polarization using a Mott polarimeter.[9]

Rate constants $k(O_2)$ and $k(\mathrm{NO})$ for exchange are derived from measurements of the dependence of the extracted electron polarization on the O_2 or NO density ρ in the flow tube and on the reaction time t. The density ρ is governed by the flow rate Q of the injected target gas and is given by $\rho=Q/\bar{v}_b A$ where $\bar{v}_b$ is the average bulk gas-flow velocity in the flow tube and A its cross-sectional area. The reaction time t is determined by the reaction length L and mean electron axial flow velocity $\bar{v}_e$ and is given by $t=L/\bar{v}_e$. The rates of change of the populations $n_\uparrow$ and $n_\downarrow$ of electrons with spin up and spin down, respectively, due to exchange are given by

$$\frac{dn_\uparrow}{dt}=-\rho k n_\uparrow+\rho k n_\downarrow\,,$$
$$\frac{dn_\downarrow}{dt}=\rho k n_\uparrow-\rho k n_\downarrow\,. \qquad (2)$$

The corresponding rate of change of the electron polarization P, defined as $P=(n_\uparrow-n_\downarrow)/(n_\uparrow+n_\downarrow)$, is therefore

$$\frac{dP}{dt}=\frac{dn_\uparrow/dt-dn_\downarrow/dt}{n_\uparrow+n_\downarrow}=-2\rho k P\,. \qquad (3)$$

Thus if P_0 is the initial electron polarization at $t=0$, that following a collision time t is given by

$$P=P_0\exp(-2\rho k t)\,, \qquad (4)$$

which can be expressed in terms of experimentally measurable quantities as

$$P=P_0\exp\left[-\frac{2kQL}{A\bar{v}_b\bar{v}_e}\right]. \qquad (5)$$

Thus, if $\bar{v}_b$, $\bar{v}_e$, and A are known, measurement of the extracted electron polarization as a function of Q and/or L permits k to be determined.

The central component of the afterglow apparatus is a Pyrex flow tube ~ 10 cm in diameter that is exhausted by a high-speed Roots pump. The helium pressure in the flow tube is typically ~ 0.08 to 0.12 torr. Helium gas entering the flow tube is excited by a microwave discharge. This excitation technique is used because it provides a preponderance of $\mathrm{He}(2\,^3S)$ metastable atoms; the ratio of $\mathrm{He}(2\,^1S)$ to $\mathrm{He}(2\,^3S)$ metastable atoms in the afterglow is $\sim$1:10. Electrons and ions produced in the discharge diffuse rapidly to the walls of the flow tube where they recombine. For the present source to extractor separation (~ 80 cm), electrons produced in the source do not contribute significantly to the extracted current.

The $2\,^3S$ atoms are optically oriented by absorption of circularly polarized 1.08-μm $2\,^3S \Longrightarrow 2\,^3P$ resonance radiation from an rf-excited high-power helium lamp, with

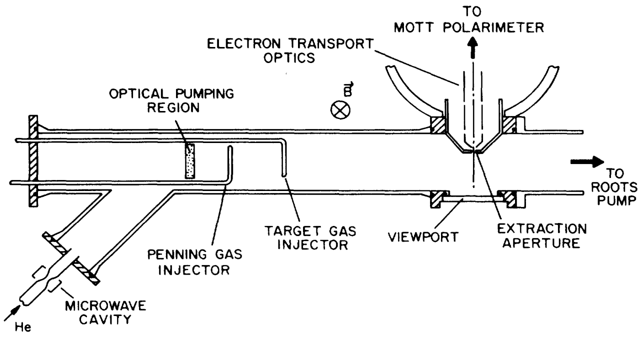

FIG. 1. Schematic diagram of the apparatus.

subsequent spontaneous decay back to the $2\,^3S$ level.[6–8] The optical pumping radiation is incident parallel to a weak (~ 1 G) external magnetic field, transverse to the axis of the flow tube, that provides a well-defined quantization axis. This field is provided by a series of coils.

The CO_2 Penning gas is introduced immediately downstream of the optical pumping region using a perforated ring injector. The electrons liberated by Penning ionization are rapidly thermalized (on a time scale of $\lesssim 50$ μsec)[10] by collisions with (principally) the injected CO_2, the pressure of which in the flow tube is typically $\sim 5\times 10^{-3}$ torr. Such collisions with CO_2, which is a spin singlet, do not degrade the electron-spin polarization.[8] Following thermalization, the polarized electrons encounter the target gas, which is introduced via a second, downstream, ring injector. The target gas-flow rate is measured using a calibrated flow meter.

The degradation in electron polarization that results from exchange is determined by extracting a fraction of the electrons from the flow tube through a differentially pumped aperture. These electrons are formed into a beam by a series of electron lenses and are directed into a retarding-potential Mott polarimeter,[9] where the component of their polarization parallel to the applied magnetic field is determined.

The average helium bulk-flow velocity $\bar{v}_b$ in the flow tube was derived from measurements of the input helium flow rate, and the flow tube pressure and cross-sectional area, yielding the value $\bar{v}_b \sim 5.4\times 10^3$ cm sec^{-1}. The flow velocity in the flow tube is, however, radially dependent. For the present operating conditions the flow is close to viscous and the radial velocity profile is approximately parabolic with velocity $\sim 2\bar{v}_b$ on axis falling to near zero at the walls.[11] Subsidiary measurements showed that the addition of small amounts of Penning or target gases does not significantly perturb the bulk helium-flow velocity.

The average electron axial velocity $\bar{v}_e$ was measured directly by modulating the polarization of the He($2\,^3S$) atoms (by rotating the quarter wave plate used as the retardation element in the circular polarizer) and observing the time (phase) delay between this applied modulation and the resultant modulation of the extracted electron polarization. This technique has the advantage that the velocity is measured under normal operating conditions without any perturbation of the charge distribution in the flow tube as would result from, say, pulsing the microwave discharge. To determine $\bar{v}_e$, the Penning gas is injected ~ 10 cm downstream of the optical pumping region and no target gas is admitted. Typical data are presented in Fig. 2. Figure 2(a) shows the polarization of the atoms in the optical pumping region; Fig. 2(b) the polarization of the extracted electrons. Because the distance from the optical pumping region to the extractor is quite large (~ 44 cm) the measured time delay Δt (~ 2.2 msec) immediately requires that $\bar{v}_e$ be greater than 2×10^4 cm sec^{-1}, which is considerably higher than the average bulk-flow velocity $\bar{v}_b$. [Data recorded using several lower polarization-modulation frequencies confirmed that the assigned time (phase) delay indicated in Fig. 2(b) is indeed correct.] The time delay Δt, however, results, in part, from the time taken for the metastable atoms to travel from the optical-pumping region to the Penning gas injector and, in part, from the time taken for the resulting Penning electrons to reach the extraction aperture. To determine the first of these times requires knowledge of the average axial metastable-atom velocity $\bar{v}_m$, which is not equal to the average bulk-flow velocity $\bar{v}_b$ because the $2\,^3S$ atom density in the flow tube is not uniform. The

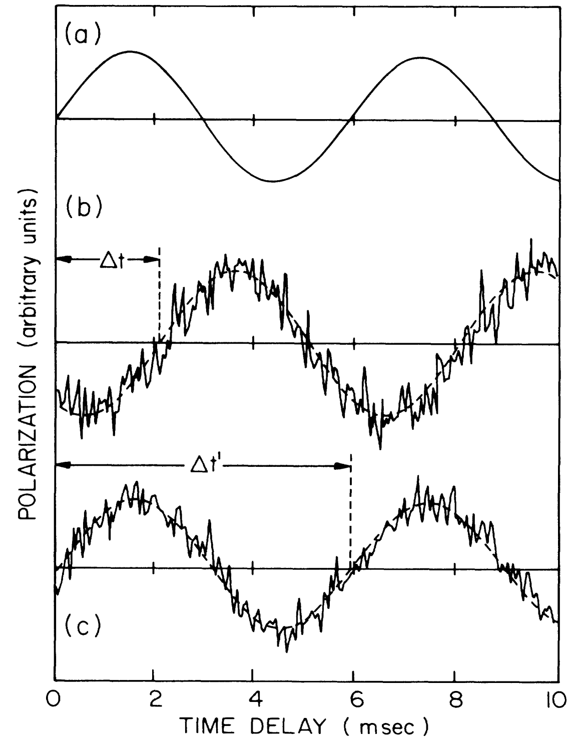

FIG. 2. (a) Polarization of the atoms in the optical-pumping region; (b) polarization of the extracted electrons observed with the Penning gas injected close to the optical pumping region; (c) polarization of the extracted electrons observed with the Penning gas injected immediately downstream of the extraction aperture. The polarization is modulated by periodically reversing the sense of circular polarization of the He($2\,^3S$) optical pumping radiation.

density is maximum on axis (where the bulk-flow velocity is highest) and falls to zero at the walls.[11] To measure $\bar{v}_m$, the Penning gas injector was repositioned ~2 cm downstream of the extraction aperture thereby allowing the metastable atoms to travel down the flow tube before being ionized in the immediate vicinity of the extraction aperture. Typical extracted electron polarization data obtained under these conditions are shown in Fig. 2(c) and the observed average metastable-atom flight time $\Delta t'$ (~6 msec) yields the value $\bar{v}_m = 7\times 10^3$ cm sec^{-1}, which is consistent with values derived by assuming that the bulk-flow velocity radial profile is parabolic (with average flow velocity $\bar{v}_b = 5.4\times 10^3$ cm sec^{-1}) and that the radial dependence of the $2\,^3S$ atom density is described by the zeroth-order Bessel function.[11] Use of $\bar{v}_m$ to obtain the transit time of the metastable atoms from the optical-pumping region to the Penning gas injector (taking into account back diffusion of the injected gas, which was investigated by monitoring the $2\,^3S$ population in the vicinity of the injector by measuring the absorption of a 1.08 μm $2\,^3S \Longrightarrow 2\,^3P$ probe beam) enables computation of the mean axial-electron velocity $\bar{v}_e$, resulting in the value $\bar{v}_e = 4\times 10^4$ cm sec^{-1}. The fact that this velocity is larger than either $\bar{v}_m$ or $\bar{v}_b$ is believed to result from electron drift due to the presence of small residual electric fields in the flow tube caused by contact potential differences between its various metal parts, all of which were electrically connected. Indeed, tests indicated that $\bar{v}_e$, and the extracted electron current, could be significantly altered by the application of small (~1 V) differential biases to different elements of the flow tube, or by changing the partial pressure of CO_2 in the flow tube. The latter observation is not unexpected because even though the density of CO_2 is small compared to that of helium it is nonetheless sufficient to significantly affect the overall electron mobility.[10] The fields required to produce drift velocities of $\sim 4\times 10^4$ cm sec^{-1} are, however, small (<10 mV cm^{-1}) and are insufficient to significantly perturb the electron-velocity distribution, which remains essentially thermal.

The dependence of the extracted electron polarization on the product LQ (with the reaction length L fixed at 30 cm) when O_2 or NO is injected into the flow tube is illustrated in Fig. 3 and displays the anticipated exponential decay. Analysis of these data, and data obtained under a variety of other operating conditions, yields the rate constants $k(O_2) = 8\pm 3.5\times 10^{-11}$ cm^{3}sec^{-1} and $k(\mathrm{NO}) = 9\pm 4\times 10^{-11}$ cm^{3}sec^{-1}. The quoted uncertainties include anticipated systematic errors, the largest of which is associated with measurement of $\bar{v}_e$. (No systematic differences were, however, noted between rate constants measured using different reaction lengths L, indicating that $\bar{v}_e$ does not change significantly with distance down the flow tube.) Data were also recorded for a number of spin-singlet target gases including Ar, N_2, and CO_2, and, as expected, no significant degradation in electron polarization due to collisions was observed.

The rate constants $k(O_2)$ and k(NO) are substantially smaller than the rate constant of $\sim 4\times 10^{-9}$ cm^{3}sec^{-1} calculated for spin change in collisions between thermal electrons and hydrogen atoms.[5] In addition, the present rate constants correspond to thermally averaged collision cross sections of $\sim 10^{-17}$ cm^2 which are very much smaller than the spin-flip cross sections of $\sim 2\times 10^{-14}$ cm^2 measured in electron–alkali-metal-atom collisions.[3,4] It is, however, not possible to identify the factors responsible for the relatively small size of the present values because, to our knowledge, no calculations of the pertinent electron–O_2 or electron–NO potential energy surfaces exist. Nonetheless, it is interesting to note that the total cross sections for thermal-electron scattering by O_2 and NO suggested by extrapolation of available experimental data [$\sim(2-5)\times 10^{-16}$ cm^2 for O_2 (Ref. 12); $\sim 10^{-15}$ cm^2 for NO (Ref. 13)] are considerably smaller than the calculated cross sections for elastic scattering of thermal electrons by hydrogen ($\sim 6\times 10^{-15}$ cm^2) (Ref. 14) or the heavier alkali-metal atoms ($\sim 6\times 10^{-14}$ cm^2).[15]

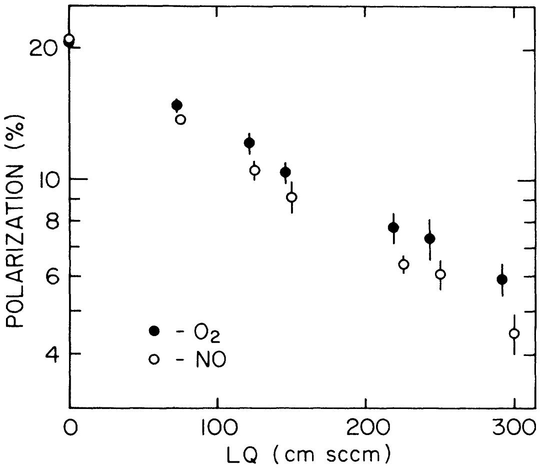

FIG. 3. The dependence of the extracted electron polarization on the product of reaction length L and target gas-flow rate Q when O_2 or NO is injected into the flow tube.

Thermal-energy electron collisions with O_2 can also result in the formation of excited O_2^- ions through the electron-attachment reaction

$$e^- + O_2(X\,^3\Sigma_g^-; v=0) \rightarrow O_2^-(X\,^2\Pi_g; v=4)\ . \tag{6}$$

The negative ions so formed are, however, unstable and, unless stabilized by a subsequent collision, will undergo rapid ($\tau \lesssim 100$ psec) autodetachment reverting to a neutral molecule plus free electron. If each of the three O_2^- π_g valence electrons detach with comparable probability the polarization of the detached electrons will, on average, be substantially less than that of those initially attached. The $v=4$ O_2^- attachment resonance is, however, narrow and at a relatively high energy (~82 meV) with respect to the ground state of neutral O_2.[16] Thus electron capture is unlikely to be the major contributor to electron exchange, and the rate constant $k_a(O_2)$ for electron attachment to O_2 should be significantly smaller than that for exchange. Studies by Hatano and co-workers[17] using microwave techniques coupled with pulsed radiolysis methods yielded values of $k_a(O_2) \sim 3 \times 10^{-11}$ cm^3 sec^{-1}, whereas measurements by Christophorou[16] using swarm techniques provided the value $k_a(O_2) \sim 2.2 \times 10^{-10}$ cm^3 sec^{-1} (for a mean electron energy of 45 meV). Possible explanations for the discrepancies between these results, based on electron attachment to Van der Waals molecules, have been discussed by Toriumi and Hatano.[17] The present measurements favor the results of Hatano and co-workers.

Thermal electron collisions with NO can result in the formation of $NO^-(X\,^3\Sigma^-)$ ions in the $v=1$ state, which lies ~ 144 meV above the ground state of neutral NO.[18] These ions, however, undergo very rapid autodetachment ($\tau \sim 0.03$ psec) precluding measurement of the corresponding electron-attachment rate constant. The present value of k(NO) provides an upper bound to the rate constant for thermal electron attachment to NO.

The research was supported by the National Science Foundation under Grant No. PHY87-17095 and by the Robert A. Welch Foundation.

---

[1] J. Kessler, *Polarized Electrons*, 2nd ed. (Springer-Velag, Berlin, 1985).

[2] G. F. Hanne, Phys. Rep. **95**, 95 (1983).

[3] H. G. Dehmelt, Phys. Rev. **109**, 381 (1958).

[4] L. C. Balling, Phys. Rev. **151**, 1 (1966).

[5] F. J. Smith, Planet. Space Sci. **14**, 929 (1966).

[6] L. G. Gray, R. S. Keiffer, J. M. Ratliff, F. B. Dunning, and G. K. Walters, Phys. Rev. A **32**, 1348 (1985).

[7] L. G. Gray, K. W. Giberson, Chu Cheng, R. S. Keiffer, F. B. Dunning, and G. K. Walters, Rev. Sci. Instrum. **54**, 271 (1983).

[8] P. J. Keliher, F. B. Dunning, M. R. O'Neill, R. D. Rundel, and G. K. Walters, Phys. Rev. A **11**, 1271 (1975).

[9] L. A. Hodge, T. J. Moravec, F. B. Dunning, and G. K. Walters, Rev. Sci. Instrum. **50**, 5 (1979).

[10] L. G. Christophorou, K. S. Gant, and J. K. Baird, Chem. Phys. Lett. **30**, 104 (1975).

[11] E. E. Ferguson, F. C. Fehsenfeld, and A. L. Schmeltekopf, Adv. At. Mol. Phys. **5**, 1 (1969).

[12] A. Zecca, R. S. Brusa, R. Grisenti, S. Oss, and C. Szmytkowski, J. Phys. B **19**, 3353 (1986).

[13] A. Zecca, I. Lazzizzera, M. Krauss, and C. E. Kuyatt, J. Chem. Phys. **61**, 4560 (1974).

[14] M. J. Seaton, Rev. Mod. Phys. **30**, 979 (1958).

[15] G. F. Drukarev, *Collisions of Electrons with Atoms and Molecules* (Plenum, New York, 1987), Chap. 6.

[16] L. G. Christophorou, Adv. in Electron. Electron Phys. **46**, 55 (1978).

[17] M. Toriumi and Y. Hatano, J. Chem. Phys. **82**, 254 (1985); **79**, 3749 (1983).

[18] H. Shimamori and H. Hotta, J. Chem. Phys. **89**, 2938 (1988).